Exact analytical formulae for linearly distributed vortex and source sheets in uence computation in 2D vortex methods

IOP Conf. Series: Journal of Physics: Conf. Series **918** (2017) 012013 doi:10.1088/1742-6596/918/1/012013

Exact analytical formulae for linearly distributed vortex and source sheets influence computation in 2D vortex methods

K S Kuzmina[1,2], I K Marchevsky[1,2] and E P Ryatina[1,2]

[1] Applied Mathematics dep., Bauman Moscow State Technical University, 2-nd Baumanskaya st., 5, 105005 Moscow, Russia

[2] Institute for System Programming of the Russian Academy of Sciences, Alexander Solzhenitsyn st. 25, 109004 Moscow, Russia

E-mail: kuz-ksen-serg@yandex.ru, iliamarchevsky@mail.ru, evgeniya.ryatina@yandex.ru

Abstract. We consider the methodology of numerical schemes development for two-dimensional vortex method. We describe two different approaches to deriving integral equation for unknown vortex sheet intensity. We simulate the velocity of the surface line of an airfoil as the influence of attached vortex and source sheets. We consider a polygonal approximation of the airfoil and assume intensity distributions of free and attached vortex sheets and attached source sheet to be approximated with piecewise constant or piecewise linear (continuous or discontinuous) functions. We describe several specific numerical schemes that provide different accuracy and have a different computational cost. The study shows that a Galerkin-type approach to solving boundary integral equation requires computing several integrals and double integrals over the panels. We obtain exact analytical formulae for all the necessary integrals, which makes it possible to raise significantly the accuracy of vortex sheet intensity computation and improve the quality of velocity and vorticity field representation, especially in proximity to the surface line of the airfoil. All the formulae are written down in the invariant form and depend only on the geometric relationship between the positions of the beginnings and ends of the panels.

1. Introduction

Vortex methods of computational fluid dynamics (CFD) [1, 2, 3, 4, 5] that belongs to the class of Lagrangian particle methods are very suitable for a wide range of engineering applications: from estimating aerodynamical coefficients for aircraft and simulating aircraft trails to dealing with hydroelastic flow-induced oscillations of structural elements and problems of industrial aerodynamics. The flows that can be simulated using vortex methods are characterized by low subsonic Mach numbers, when the effects of flow compressibility can be neglected. Efficient parallel implementations of vortex methods, adapted for computations on both CPUs and GPUs, makes it possible to solve certain hydrodynamic and hydroelastic problems much faster in comparison with traditional mesh methods [6].

In the 2D case the most efficient modifications of vortex methods are able to simulate viscous incompressible flows that are described by the Navier — Stokes equations [4, 5, 7, 8, 9]. We

consider the problem in the most general case, when there is an incident flow and an airfoil of an arbitrary shape, which can be movable and/or deformable.

Modifications of vortex methods to simulate 3D flows are also known, but there are fundamental differences between 2D and 3D flows. The main feature of 2D flows is that the vorticity vector is always perpendicular to the plane of the flow. It significantly simplifies the solution procedure for 2D problems. However, in a number of applications dealing with solving coupled aerohydrodynamic and aerohydroelastic problems a flat cross-sections approach is applicable, which reduces a 3D problem to a much simpler problem of simulating 2D flows around one or several cross-sections of the structure considered. Moreover, despite the differences between mathematical formulations of 2D and 3D problems and their properties, a number of basic approaches that proved to present an advantage when solving 2D problems may be successfully used in the 3D case in much the same manner. This fact, in turn, is a powerful stimulus for development of vortex methods.

2. Velocity field reconstruction

Vortex methods of simulating the flow around airfoils are based on the principle that was discovered by Professor N.E. Zhukovsky. According to this principle, it is possible to replace a stationary airfoil by an attached vortex layer placed on its surface line [10]. Conformal mapping technique can be used to find the vortex sheet intensity for airfoils of primitive shapes; such solutions can serve as benchmarks for verification of the numerical schemes being developed.

When solving the Navier — Stokes equations, Zhukovsky's classical ideas remain correct, but such vortex sheet is free instead of being attached, and according to Lighthill's approach [11], it can be considered as a result of the vorticity flux acting on the airfoil surface line K during an infinitesimal time period. It means that the vorticity concentrated in this vortex sheet with the intensity $\gamma(\boldsymbol{r})$, $\boldsymbol{r} \in K$ is not connected with the airfoil and, after being generated on its surface line, it becomes part of the vortex wake and moves in the flow according to the governing equations.

If the airfoil is movable and/or deformable, we should introduce in addition to the free vortex sheet mentioned above, *i.e.* attached vortex sheet with the intensity γ^{att} and attached source sheet with the intensity q^{att} [12, 13]. For simplicity, we assume that the velocity $\boldsymbol{V}_K(\boldsymbol{r})$ is known for an arbitrary point on the airfoil surface line K, so the intensities of the attached sheets can be found explicitly:

$$\gamma^{att}(\boldsymbol{r}) = \boldsymbol{V}_K(\boldsymbol{r}) \cdot \boldsymbol{\tau}(\boldsymbol{r}), \qquad q^{att}(\boldsymbol{r}) = \boldsymbol{V}_K(\boldsymbol{r}) \cdot \boldsymbol{n}(\boldsymbol{r}), \qquad \boldsymbol{r} \in K,$$

where $\boldsymbol{\tau}(\boldsymbol{r})$ and $\boldsymbol{n}(\boldsymbol{r})$ are tangent and normal unit vectors to the airfoil surface line, respectively.

In order to compute the flow velocity for an arbitrary point of the flow domain, we use a generalized Biot — Savart law [14]:

$$\boldsymbol{V}(\boldsymbol{r}) = \boldsymbol{V}_\infty + \frac{1}{2\pi}\int_S \frac{\boldsymbol{\Omega}(\boldsymbol{\xi}) \times (\boldsymbol{r} - \boldsymbol{\xi})}{|\boldsymbol{r} - \boldsymbol{\xi}|^2} dS_\xi + \frac{1}{2\pi}\oint_K \frac{\boldsymbol{\gamma}(\boldsymbol{\xi}) \times (\boldsymbol{r} - \boldsymbol{\xi})}{|\boldsymbol{r} - \boldsymbol{\xi}|^2} dl_\xi + \\ + \frac{1}{2\pi}\oint_K \frac{\boldsymbol{\gamma}^{att}(\boldsymbol{\xi}) \times (\boldsymbol{r} - \boldsymbol{\xi})}{|\boldsymbol{r} - \boldsymbol{\xi}|^2} dl_\xi + \frac{1}{2\pi}\oint_K \frac{q^{att}(\boldsymbol{\xi})(\boldsymbol{r} - \boldsymbol{\xi})}{|\boldsymbol{r} - \boldsymbol{\xi}|^2} dl_\xi. \quad (1)$$

Here S is the flow domain; attached and free vortex sheet intensity vectors and the vorticity vector are

$$\boldsymbol{\gamma}^{att}(\boldsymbol{\xi}) = \gamma^{att}(\boldsymbol{\xi})\,\boldsymbol{k}, \qquad \boldsymbol{\gamma}(\boldsymbol{\xi}) = \gamma(\boldsymbol{\xi})\,\boldsymbol{k}, \qquad \boldsymbol{\Omega}(\boldsymbol{\xi}) = \Omega(\boldsymbol{\xi})\,\boldsymbol{k}, \quad (2)$$

respectively, where $\boldsymbol{k}$ is a unit vector orthogonal to the flow plane; on the airfoil surface $\boldsymbol{n}(\boldsymbol{r}) \times \boldsymbol{\tau}(\boldsymbol{r}) = \boldsymbol{k}$.

The flow velocity limit value on the surface line of the airfoil cannot be computed directly by using (1), because $\boldsymbol{V}(\boldsymbol{r})$ has a jump discontinuity there [1]. The following formula should be used to compute it:

$$\boldsymbol{V}_-(\boldsymbol{r}) = \boldsymbol{V}(\boldsymbol{r}) - \frac{\gamma(\boldsymbol{r}) - \gamma^{att}(\boldsymbol{r})}{2}\boldsymbol{\tau}(\boldsymbol{r}) + \frac{q^{att}(\boldsymbol{r})}{2}\boldsymbol{n}(\boldsymbol{r}), \qquad \boldsymbol{r} \in K. \tag{3}$$

3. Integral equation

In order to solve the problem of flow simulation around an airfoil we need to find the distribution of free vortex sheet intensity over the surface line. We can do it by satisfying the boundary condition on the surface line:

$$\boldsymbol{V}_-(\boldsymbol{r}) = \boldsymbol{V}_K(\boldsymbol{r}), \qquad \boldsymbol{r} \in K. \tag{4}$$

It can be shown that the equalities between normal components of velocities

$$\boldsymbol{V}_-(\boldsymbol{r}) \cdot \boldsymbol{n}(\boldsymbol{r}) = \boldsymbol{V}_K(\boldsymbol{r}) \cdot \boldsymbol{n}(\boldsymbol{r}), \qquad \boldsymbol{r} \in K, \tag{5}$$

or between their tangent components

$$\boldsymbol{V}_-(\boldsymbol{r}) \cdot \boldsymbol{\tau}(\boldsymbol{r}) = \boldsymbol{V}_K(\boldsymbol{r}) \cdot \boldsymbol{\tau}(\boldsymbol{r}), \qquad \boldsymbol{r} \in K, \tag{6}$$

are two equivalent sufficient conditions for satisfying the equality (4).

However, the resulting integral equations with respect to the unknown $\gamma(\boldsymbol{r})$, which can be derived from (5) and (6) after substituting the expression (3) for the limit value of velocity in those, have quite different properties.

In the framework of "classical" implementations of vortex methods, the boundary condition is used in form (5), and the governing integral equation, which is a first kind equation in this case, can be written down as

$$\frac{1}{2\pi}\oint_K Q_n(\boldsymbol{r}, \boldsymbol{\xi})\gamma(\boldsymbol{\xi})\, dl_\xi = f_n(\boldsymbol{r}), \qquad \boldsymbol{r} \in K, \tag{7}$$

where the kernel $Q_n(\boldsymbol{r}, \boldsymbol{\xi})$ is an unbounded (singular) one of Hilbert-type

$$Q_n(\boldsymbol{r}, \boldsymbol{\xi}) = \frac{\boldsymbol{k} \times (\boldsymbol{r} - \boldsymbol{\xi})}{|\boldsymbol{r} - \boldsymbol{\xi}|^2} \cdot \boldsymbol{n}(\boldsymbol{r}) = -\frac{\boldsymbol{\tau}(\boldsymbol{r}) \cdot (\boldsymbol{r} - \boldsymbol{\xi})}{|\boldsymbol{r} - \boldsymbol{\xi}|^2},$$

and the right-hand side $f_n(\boldsymbol{r})$ is a known function which depends on the shape of the airfoil, incident flow velocity, velocity of the airfoil itself and vorticity distribution in the flow domain:

$$f_n(\boldsymbol{r}) = -\frac{1}{2}q^{att}(\boldsymbol{r}) - \boldsymbol{n}(\boldsymbol{r}) \cdot \left(\boldsymbol{V}_\infty - \boldsymbol{V}_K(\boldsymbol{r}) + \frac{1}{2\pi}\int_S \frac{\boldsymbol{\Omega}(\boldsymbol{\xi}) \times (\boldsymbol{r} - \boldsymbol{\xi})}{|\boldsymbol{r} - \boldsymbol{\xi}|^2} dS_\xi + \right.$$
$$\left. + \frac{1}{2\pi}\oint_K \frac{\boldsymbol{\gamma}^{att}(\boldsymbol{\xi}) \times (\boldsymbol{r} - \boldsymbol{\xi})}{|\boldsymbol{r} - \boldsymbol{\xi}|^2} dl_\xi + \frac{1}{2\pi}\oint_K \frac{q^{att}(\boldsymbol{\xi})(\boldsymbol{r} - \boldsymbol{\xi})}{|\boldsymbol{r} - \boldsymbol{\xi}|^2} dl_\xi \right). \tag{8}$$

An approximate numerical solution of equation (7) requires specific quadrature formulae; in the simplest case, those can be discrete vortex type quadrature formulae [1], which permit us to select the principal value of the corresponding singular integral in the Cauchy sense.

If we construct the numerical scheme of our vortex method on the basis of a "tangent" approach (6), the integral equation transforms into the second kind equation

$$\frac{1}{2\pi}\oint_K Q_\tau(\boldsymbol{r}, \boldsymbol{\xi})\gamma(\boldsymbol{\xi})\, dl_\xi - \frac{1}{2}\gamma(\boldsymbol{r}) = f_\tau(\boldsymbol{r}), \qquad \boldsymbol{r} \in K, \tag{9}$$

where the kernel

$$Q_\tau(\boldsymbol{r},\,\boldsymbol{\xi}) = \frac{\boldsymbol{k}\times(\boldsymbol{r}-\boldsymbol{\xi}\,)}{|\boldsymbol{r}-\boldsymbol{\xi}\,|^2}\cdot\boldsymbol{\tau}(\boldsymbol{r}) = \frac{\boldsymbol{n}(\boldsymbol{r})\cdot(\boldsymbol{r}-\boldsymbol{\xi}\,)}{|\boldsymbol{r}-\boldsymbol{\xi}\,|^2}$$

is now a uniformly bounded function when K is a smooth curve, and unbounded only in proximity to angle points or sharp edges of a non-smooth airfoil surface line K, and the right-hand side has the following form:

$$f_\tau(\boldsymbol{r}) = -\frac{1}{2}\gamma^{att}(\boldsymbol{r}) - \boldsymbol{\tau}(\boldsymbol{r})\cdot\left(\boldsymbol{V}_\infty - \boldsymbol{V}_K(\boldsymbol{r}) + \frac{1}{2\pi}\int_S \frac{\boldsymbol{\Omega}(\boldsymbol{\xi})\times(\boldsymbol{r}-\boldsymbol{\xi}\,)}{|\boldsymbol{r}-\boldsymbol{\xi}\,|^2}dS_\xi + \right.$$
$$\left. + \frac{1}{2\pi}\oint_K \frac{\boldsymbol{\gamma}^{att}(\boldsymbol{\xi})\times(\boldsymbol{r}-\boldsymbol{\xi}\,)}{|\boldsymbol{r}-\boldsymbol{\xi}\,|^2}dl_\xi + \frac{1}{2\pi}\oint_K \frac{q^{att}(\boldsymbol{\xi})(\boldsymbol{r}-\boldsymbol{\xi}\,)}{|\boldsymbol{r}-\boldsymbol{\xi}\,|^2}dl_\xi\right). \quad (10)$$

Results of numerical experiments show that the "tangent" approach, which corresponds to numerical solving the equation (9), makes it possible to raise the accuracy of vortex sheet intensity computation significantly. Nevertheless, in some cases a "normal" approach (7) can also be useful.

We should note that both equations (7) and (9) have an infinite set of solutions. In order to select a physically plausible unique solution, an additional condition should be added, which in most cases corresponds to given value of the integral from solution over the surface line:

$$\oint_K \gamma(\boldsymbol{\xi})dl_\xi = \Gamma. \quad (11)$$

4. Problem discretization

When solving a problem using vortex methods, the vortex wake is normally simulated by discrete vortex-type singularities (vortex elements):

$$\Omega(\boldsymbol{r},\,t) = \sum_{w=1}^{n}\Gamma_w\tilde{\delta}(\boldsymbol{r}-\boldsymbol{r}_w). \quad (12)$$

Here n is the number of vortex elements, Γ_w and $\boldsymbol{r}_w$ are intensities and positions of vortex elements, respectively, and $\tilde{\delta}$ is a two-dimensional Dirac delta function. Taking into account (2) and (12), we obtain for the term, which corresponds to the integral over the flow domain in right-hand side functions (8) and (10)

$$\frac{1}{2\pi}\int_S \frac{\boldsymbol{\Omega}(\boldsymbol{\xi})\times(\boldsymbol{r}-\boldsymbol{\xi}\,)}{|\boldsymbol{r}-\boldsymbol{\xi}\,|^2}dS_\xi = \sum_{w=1}^{n}\frac{\Gamma_w}{2\pi}\frac{\boldsymbol{k}\times(\boldsymbol{r}-\boldsymbol{r}_w)}{|\boldsymbol{r}-\boldsymbol{r}_w|^2}.$$

The simplest way to discretize the surface line K of the airfoil is to approximate it by a polygon consisting of N rectilinear segments K_i, which we call hereinafter "panels". Let us denote panel lengthes by L_i, their normal and tangent unit vectors by $\boldsymbol{n}_i$ and $\boldsymbol{\tau}_i$, respectively, $i = 1,\,\ldots,\,N$. Now all the integrals over the surface line in the previous formulae can be written down as sums of integrals over separate panels.

We then consider the intensity distributions of the free and attached vortex sheets and source sheet over the surface line to be piecewise-linear functions:

$$\gamma(\boldsymbol{r}) = \sum_{i=1}^{N}\Big(\gamma_i\phi_0^i(\boldsymbol{r}) + \delta_i\phi_1^i(\boldsymbol{r})\Big), \qquad \gamma^{att}(\boldsymbol{r}) = \sum_{i=1}^{N}\Big(\gamma_i^{att}\phi_0^i(\boldsymbol{r}) + \delta_i^{att}\phi_1^i(\boldsymbol{r})\Big),$$
$$q^{att}(\boldsymbol{r}) = \sum_{i=1}^{N}\Big(q_i^{att}\phi_0^i(\boldsymbol{r}) + p_i^{att}\phi_1^i(\boldsymbol{r})\Big), \qquad \boldsymbol{r}\in K.$$

Here $\phi_j^i(\boldsymbol{r})$, $i = 1, \ldots, N$, $j = 0, 1$, is a set of basis functions:

$$\phi_0^i(\boldsymbol{r}) = \begin{cases} 1, & \boldsymbol{r} \in K_i, \\ 0, & \boldsymbol{r} \notin K_i; \end{cases} \qquad \phi_1^i(\boldsymbol{r}) = \begin{cases} \dfrac{(\boldsymbol{r} - \boldsymbol{c}_i) \cdot \boldsymbol{\tau}_i}{L_i}, & \boldsymbol{r} \in K_i, \\ 0, & \boldsymbol{r} \notin K_i, \end{cases} \tag{13}$$

where $\boldsymbol{c}_i$ is the center of the i-th panel, and the unit tangent vector $\boldsymbol{\tau}_i$ is directed from the beginning to the end of the i-th panel. So, the basis function ϕ_0^i is constant over the panel, while the basis function ϕ_1^i varies linearly from $-1/2$ to $1/2$ along the i-th panel.

Different approaches can be used to construct a numerical solution $\gamma(\boldsymbol{r})$ over the whole airfoil surface line, as well as to approximate $\gamma^{att}(\boldsymbol{r})$ and $q^{att}(\boldsymbol{r})$. In order to find unknown coefficients in the representation of the solution, we use a Galerkin-type approach: the residual of equations (7) or (9) should be orthogonal to projection functions $\{\psi_k(\boldsymbol{r})\}$.

A number of possible ways to numerical solution of the equation (9) are briefly described below.

(i) In the simplest case a piecewise-constant discontinuous approximation can be considered, so $\delta_i = 0$, $\delta_i^{att} = 0$ and $p_i^{att} = 0$ for all $i = 1, \ldots, N$. So γ_i^{att} and q_i^{att} should be chosen as average values of the corresponding intensities over the panels:

$$\gamma_i^{att} = \frac{1}{L_i} \int_{K_i} \gamma^{att}(\boldsymbol{r}) dl_\xi \approx \boldsymbol{V}_K(\boldsymbol{c}_i) \cdot \boldsymbol{\tau}_i, \qquad q_i^{att} = \frac{1}{L_i} \int_{K_i} q^{att}(\boldsymbol{r}) dl_\xi \approx \boldsymbol{V}_K(\boldsymbol{c}_i) \cdot \boldsymbol{n}_i.$$

As a result, the unknown distribution depends only on N unknown values γ_i, which can be found from conditions of orthogonality to a set of projection functions $\{\psi_k(\boldsymbol{r})\} = \{\phi_0^k(\boldsymbol{r})\}_{k=1}^N$.
This approximation makes it possicle to achieve second-order accuracy with respect to the average values γ_i of the free vortex sheet intensity over the panels and first-order accuracy in the L_1 norm.
Publication [15] presents a description of this approach and its comparison with less accurate ones, as well as all the necessary formulae for computations.

(ii) Approximations of the solution $\gamma(\boldsymbol{r})$ and known distributions $\gamma^{att}(\boldsymbol{r})$ and $q^{att}(\boldsymbol{r})$ remain the same as in the previous case, but unknown values γ_i, $i = 1, \ldots, N$ can be found from collocation-type conditions, which means that the residual of equations (7) or (9) is equal to zero only at certain selected points on the surface line, as a rule, at the centers of the panels.
This modification is equivalent to the previous one, if $\{\psi_k(\boldsymbol{r})\} = \{\delta(\boldsymbol{r} - \boldsymbol{c}_k)\}_{k=1}^N$, where δ is a Dirac delta-function:

$$\int_{K_i} g(\boldsymbol{r}) \psi_i(\boldsymbol{r}) dl_\xi = g(\boldsymbol{c}_i), \qquad i = 1, \ldots, N.$$

(iii) In the most complicated case, piecewise-linear discontinuous approximation are considered, so the resulting solution depends on $2N$ unknown values γ_i and δ_i, $i = 1, \ldots, N$, which can be found from the same approach with the only difference that now the set of projection functions consists of functions $\{\phi_0^i(\boldsymbol{r})\}_{i=1}^N$ and $\{\phi_1^i(\boldsymbol{r})\}_{i=1}^N$ together. This method provides the second-order accuracy with respect to the average values of the free vortex sheet intensity γ_i and to the vortex sheet intensity distribution in the L_1 norm.
Paper [16] presents a description of this method and the results of solving test problems for airfoils of simple shapes (elliptical and the Zhukovsky wing).

(iv) A "finite element-type" approach provides a continuous piecewise-linear solution approximation. The basis functions in this case are first-order linear shape functions, which can be easily constructed from (13):

$$\hat{\phi}^i(\boldsymbol{r}) = \begin{cases} \dfrac{1}{2}\phi_0^{i-1}(\boldsymbol{r}) + \phi_1^{i-1}(\boldsymbol{r}), & \boldsymbol{r} \in K_{i-1}, \\ \dfrac{1}{2}\phi_0^{i}(\boldsymbol{r}) - \phi_1^{i}(\boldsymbol{r}), & \boldsymbol{r} \in K_i, \qquad i = 1, \ldots, N, \quad K_0 \equiv K_N, \end{cases}$$

and finally

$$\gamma(\boldsymbol{r}) = \sum_{i=1}^{N} \hat{\gamma}_i \hat{\phi}^i(\boldsymbol{r}),$$

where unknown values $\hat{\gamma}_i$ correspond to the intensities of the free vortex sheet at the beginnings of the panels. In order to determine them, as in the FEM, we select projection functions to be equal to the shape functions: $\{\psi_k(\boldsymbol{r})\} = \{\hat{\phi}^k(\boldsymbol{r})\}_{k=1}^N$.
If the exact solution is continuous, this modification provides second-order accuracy, same as the previous one, but the dimension of the problem is twice as small and is equal to the number of panels N. But if the airfoil has sharp edges or angle point, it leads to incorrect behavior of the numerical solution in proximity to such points.
Note, that in the framework of the FEM approach Dirac delta functions can also be used as projection ones.

(v) A "hybrid" schemes involves a piecewise-linear solution, which is discontinuous only at N_d chosen points, and continuous at all others. The number of unknown values here is $N + N_d$, all basis functions can be expressed through ϕ_0^i and ϕ_1^i. Projection functions again coincide with the basis ones.
Numerical experiments show that this approach remains correct and provides second-order accuracy for airfoils with angle points and sharp edges when they are marked as discontinuity points. This scheme may be called "cost-efficient" because the dimension of the resulting matrix is $N + N_d$, which is much smaller than $2N$.

Some other modifications are also possible for solving both equations (7) and (9) numerically, but the main principles of constructing those remain the same.

The easiest way to take into account the additional condition (11) is to add one extra "regularization" variable R to all the equations in the resulting linear system and solve it together with the linear equation, which follows from (11) after discretization. Another possible approach is to find pseudo-solution of a non-regularized linear system.

5. Analytical computation of integrals

In order to compute matrix and right-hand side coefficients for discrete analogues of the equations (7) and (9) according to numerical schemes described in the previous section or some other schemes that are constructed using Galerkin-type approach with piecewise-constant and piecewise-linear basis and projection functions, it is necessary to compute the following integrals (note that $\phi_0^i \equiv 1$ over the i-th panel):

$$\boldsymbol{I}_j^0(\boldsymbol{r}) = \int_{K_j} \boldsymbol{Q}(\boldsymbol{r} - \boldsymbol{\xi}) dl_\xi, \qquad \boldsymbol{I}_j^1(\boldsymbol{r}) = \int_{K_j} \boldsymbol{Q}(\boldsymbol{r} - \boldsymbol{\xi}) \phi_1^j(\boldsymbol{\xi}) dl_\xi,$$

$$\boldsymbol{I}_{ij}^{00} = \int_{K_i} dl_r \int_{K_j} \boldsymbol{Q}(\boldsymbol{r} - \boldsymbol{\xi}) dl_\xi, \qquad \boldsymbol{I}_{ij}^{01} = \int_{K_i} dl_r \int_{K_j} \boldsymbol{Q}(\boldsymbol{r} - \boldsymbol{\xi}) \phi_1^j(\boldsymbol{\xi}) dl_\xi,$$

$$\boldsymbol{I}_{ij}^{10} = \int_{K_i} dl_r \int_{K_j} \boldsymbol{Q}(\boldsymbol{r} - \boldsymbol{\xi}) \phi_1^i(\boldsymbol{r}) dl_\xi, \qquad \boldsymbol{I}_{ij}^{11} = \int_{K_i} dl_r \int_{K_j} \boldsymbol{Q}(\boldsymbol{r} - \boldsymbol{\xi}) \phi_1^i(\boldsymbol{r}) \phi_1^j(\boldsymbol{\xi}) dl_\xi.$$

We write down these integrals with a "vector kernel"

$$\boldsymbol{Q}(\boldsymbol{r}-\boldsymbol{\xi}) = \frac{\boldsymbol{r}-\boldsymbol{\xi}}{|\boldsymbol{r}-\boldsymbol{\xi}\,|^2},$$

in order to have the possibility to adapt them easily to computing the integrals in equations (7) and (9), taking into account the expressions (8) and (10) for their right-hand sides. It should be noted that the kernel $\boldsymbol{Q}$ is anti-symmetric:

$$\boldsymbol{Q}(\boldsymbol{r}-\boldsymbol{\xi}) = -\boldsymbol{Q}(\boldsymbol{\xi}-\boldsymbol{r}),$$

so all other necessary integrals can be expressed through the ones considered.

5.1. Computation of integrals $\boldsymbol{I}_j^0(\boldsymbol{r})$ and $\boldsymbol{I}_j^1(\boldsymbol{r})$
Figure 1 shows the j-th panel of the airfoil and the point $\boldsymbol{r}$ and introduces several auxiliary vectors for computation of the integrals $\boldsymbol{I}_j^0(\boldsymbol{r})$ and $\boldsymbol{I}_j^1(\boldsymbol{r})$: vectors $\boldsymbol{s}$ and $\boldsymbol{p}$ join the beginning and the end of the j-th panel to the point $\boldsymbol{r}$, respectively.

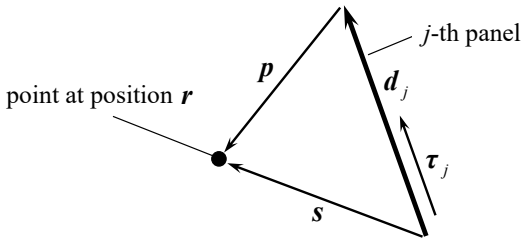

Figure 1. The j-th panel and auxiliary vectors

Employing these vectors after some transformations it is possible to write down the following formulae:

$$\boldsymbol{I}_j^0(\boldsymbol{r}) = \int_{K_j} \boldsymbol{Q}(\boldsymbol{r}-\boldsymbol{\xi})dl_\xi = \alpha\boldsymbol{u}_0 \times \boldsymbol{k} + \lambda\boldsymbol{u}_0,$$

$$\boldsymbol{I}_j^1(\boldsymbol{r}) = \int_{K_j} \boldsymbol{Q}(\boldsymbol{r}-\boldsymbol{\xi})\phi_1^j(\boldsymbol{\xi})dl_\xi = \alpha\boldsymbol{u}_1 \times \boldsymbol{k} + \lambda\boldsymbol{u}_1 - \boldsymbol{\tau}_j.$$

Here we denote

$$\boldsymbol{u}_0 = \boldsymbol{\omega}(\boldsymbol{\tau}_j,\, \boldsymbol{\tau}_j,\, \boldsymbol{\tau}_j) = \boldsymbol{\tau}_j, \quad \boldsymbol{u}_1 = \frac{1}{2|\boldsymbol{d}_j|}\boldsymbol{\omega}(\boldsymbol{p}+\boldsymbol{s},\, \boldsymbol{\tau}_j,\, \boldsymbol{\tau}_j),$$
$$\alpha = \angle(\boldsymbol{p},\, \boldsymbol{s}), \quad \lambda = \ln\frac{|\boldsymbol{s}|}{|\boldsymbol{p}|},$$

where

$$\boldsymbol{\omega}(\boldsymbol{a},\, \boldsymbol{b},\, \boldsymbol{c}) = (\boldsymbol{a}\cdot\boldsymbol{b})\,\boldsymbol{c} + (\boldsymbol{a}\times\boldsymbol{b})\times\boldsymbol{c}, \qquad \angle(\boldsymbol{p},\, \boldsymbol{s}) = \mathrm{Arg}\big(\boldsymbol{p}\cdot\boldsymbol{s} + i(\boldsymbol{p}\,\boldsymbol{s}\,\boldsymbol{k})\big). \tag{14}$$

5.2. Computation of integrals $\boldsymbol{I}_{ij}^{00}$, $\boldsymbol{I}_{ij}^{01}$, $\boldsymbol{I}_{ij}^{10}$ and $\boldsymbol{I}_{ij}^{11}$
Figure 2 shows the i-th and j-th panels and introduces auxiliary vectors similarly to the previous case: vectors $\boldsymbol{d}_i$ and $\boldsymbol{d}_j$ are codirectional with the i-th and j-th panels; vectors $\boldsymbol{s}_1$ and $\boldsymbol{s}_2$ join the beginning of the j-th panel with the end and the beginning of the i-th panel, respectively;

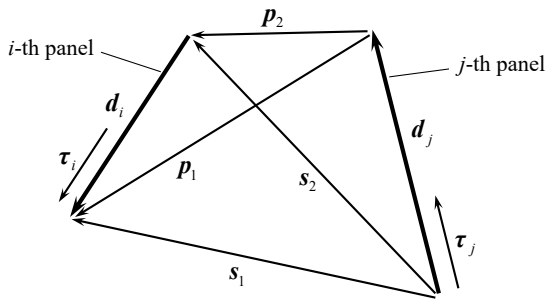

Figure 2. The i-th and j-th panels and auxiliary vectors

vectors $\boldsymbol{p}_1$ and $\boldsymbol{p}_2$ join the end of the j-th panel with the end and the beginning of the i-th panel, respectively.

These vectors enabled us to derive the following formulae after a number of transformations performed in the *Wolfram Mathematica* computer algebra system:

$$\boldsymbol{I}_{ij}^{00} = \int_{K_i} dl_r \int_{K_j} \boldsymbol{Q}(\boldsymbol{r}-\boldsymbol{\xi}) dl_\xi = (\alpha_1\boldsymbol{v}_1 + \alpha_2\boldsymbol{v}_2 + \alpha_3\boldsymbol{v}_3) \times \boldsymbol{k} + (\lambda_1\boldsymbol{v}_1 + \lambda_2\boldsymbol{v}_2 + \lambda_3\boldsymbol{v}_3),$$

$$\begin{aligned}\boldsymbol{I}_{ij}^{01} &= \int_{K_i} dl_r \int_{K_j} \boldsymbol{Q}(\boldsymbol{r}-\boldsymbol{\xi})\phi_1^j(\boldsymbol{\xi}) dl_\xi = \\ &= \big((\alpha_1+\alpha_3)\boldsymbol{v}_4 + \alpha_3\boldsymbol{v}_5\big) \times \boldsymbol{k} + \big((\lambda_1+\lambda_3)\boldsymbol{v}_4 + \lambda_3\boldsymbol{v}_5\big) + \frac{1}{2}|\boldsymbol{d}_j|\boldsymbol{\tau}_i,\end{aligned}$$

$$\begin{aligned}\boldsymbol{I}_{ij}^{10} &= \int_{K_i} dl_r \int_{K_j} \boldsymbol{Q}(\boldsymbol{r}-\boldsymbol{\xi})\phi_1^i(\boldsymbol{r}) dl_\xi = \\ &= \big((\alpha_1+\alpha_3)\boldsymbol{v}_6 + \alpha_4\boldsymbol{v}_7\big) \times \boldsymbol{k} + \big((\lambda_1+\lambda_3)\boldsymbol{v}_6 + \lambda_4\boldsymbol{v}_7\big) - \frac{1}{2}|\boldsymbol{d}_i|\boldsymbol{\tau}_j,\end{aligned}$$

$$\begin{aligned}\boldsymbol{I}_{ij}^{11} &= \int_{K_i} dl_r \int_{K_j} \boldsymbol{Q}(\boldsymbol{r}-\boldsymbol{\xi})\phi_1^i(\boldsymbol{r})\phi_1^j(\boldsymbol{\xi}) dl_\xi = \\ &= \big((\alpha_1+\alpha_3)\boldsymbol{v}_8 + \alpha_4\boldsymbol{v}_9 + \alpha_3\boldsymbol{v}_{10}\big) \times \boldsymbol{k} + \big((\lambda_1+\lambda_3)\boldsymbol{v}_8 + \lambda_4\boldsymbol{v}_9 + \lambda_3\boldsymbol{v}_{10}\big) + \\ &+ \frac{1}{12}\big(|\boldsymbol{d}_j|\boldsymbol{\tau}_i + |\boldsymbol{d}_i|\boldsymbol{\tau}_j - 2\boldsymbol{\omega}(\boldsymbol{s}_1, \boldsymbol{\tau}_i, \boldsymbol{\tau}_j)\big).\end{aligned}$$

Here we have introduced the following notations, taking into account (14):

$$\alpha_1 = \angle(\boldsymbol{s}_2, \boldsymbol{s}_1), \quad \alpha_2 = \angle(\boldsymbol{s}_2, \boldsymbol{p}_1), \quad \alpha_3 = \angle(\boldsymbol{p}_1, \boldsymbol{p}_2), \quad \alpha_4 = \alpha_2 + \alpha_3 = \angle(\boldsymbol{s}_2, \boldsymbol{p}_2)$$

$$\lambda_1 = \ln\frac{|\boldsymbol{s}_1|}{|\boldsymbol{s}_2|}, \quad \lambda_2 = \ln\frac{|\boldsymbol{p}_1|}{|\boldsymbol{s}_2|}, \quad \lambda_3 = \ln\frac{|\boldsymbol{p}_2|}{|\boldsymbol{p}_1|}, \quad \lambda_4 = \lambda_2 + \lambda_3 = \ln\frac{|\boldsymbol{p}_2|}{|\boldsymbol{s}_2|},$$

$$\boldsymbol{v}_1 = \boldsymbol{\omega}(\boldsymbol{s}_1, \boldsymbol{\tau}_i, \boldsymbol{\tau}_j), \quad \boldsymbol{v}_2 = -\boldsymbol{\omega}(\boldsymbol{d}_i, \boldsymbol{\tau}_i, \boldsymbol{\tau}_j), \quad \boldsymbol{v}_3 = \boldsymbol{\omega}(\boldsymbol{p}_2, \boldsymbol{\tau}_i, \boldsymbol{\tau}_j),$$

$$\boldsymbol{v}_4 = -\frac{1}{2|\boldsymbol{d}_i|}\big(((\boldsymbol{s}_1+\boldsymbol{s}_2)\cdot\boldsymbol{\tau}_i)\boldsymbol{\omega}(\boldsymbol{s}_1, \boldsymbol{\tau}_i, \boldsymbol{\tau}_j) - |\boldsymbol{s}_1|^2\boldsymbol{\tau}_j\big), \quad \boldsymbol{v}_5 = \frac{|\boldsymbol{d}_j|}{2|\boldsymbol{d}_i|}\boldsymbol{\omega}(\boldsymbol{s}_1+\boldsymbol{p}_2, \boldsymbol{\tau}_i, \boldsymbol{\tau}_i),$$

$$\boldsymbol{v}_6 = \frac{1}{2|\boldsymbol{d}_j|}\big(((\boldsymbol{p}_1+\boldsymbol{s}_1)\cdot\boldsymbol{\tau}_j)\boldsymbol{\omega}(\boldsymbol{s}_1, \boldsymbol{\tau}_i, \boldsymbol{\tau}_j) - |\boldsymbol{s}_1|^2\boldsymbol{\tau}_i\big), \quad \boldsymbol{v}_7 = -\frac{|\boldsymbol{d}_i|}{2|\boldsymbol{d}_j|}\boldsymbol{\omega}(\boldsymbol{s}_1+\boldsymbol{p}_2, \boldsymbol{\tau}_j, \boldsymbol{\tau}_j),$$

$$\boldsymbol{v}_8 = \frac{1}{12|\boldsymbol{d}_i||\boldsymbol{d}_j|}\Big(2\big(\boldsymbol{s}_1\cdot\boldsymbol{\omega}(\boldsymbol{s}_1-3\boldsymbol{p}_2, \boldsymbol{\tau}_i, \boldsymbol{\tau}_j)\big)\boldsymbol{\omega}(\boldsymbol{s}_1, \boldsymbol{\tau}_i, \boldsymbol{\tau}_j) - |\boldsymbol{s}_1|^2(\boldsymbol{s}_1-3\boldsymbol{p}_2)\Big) - \frac{1}{4}\boldsymbol{\omega}(\boldsymbol{s}_1, \boldsymbol{\tau}_i, \boldsymbol{\tau}_j),$$

$$\boldsymbol{v}_9 = -\frac{1}{12}\frac{|\boldsymbol{d}_i|}{|\boldsymbol{d}_j|}\boldsymbol{\omega}(\boldsymbol{d}_i, \boldsymbol{\tau}_j, \boldsymbol{\tau}_j), \quad \boldsymbol{v}_{10} = -\frac{1}{12}\frac{|\boldsymbol{d}_j|}{|\boldsymbol{d}_i|}\boldsymbol{\omega}(\boldsymbol{d}_j, \boldsymbol{\tau}_i, \boldsymbol{\tau}_i).$$

If $i = j$, then the corresponding integrals are singular, and their limit values, which are required to compute matrix coefficients and right-hand sides, are equal to zero:

$$\boldsymbol{I}_{ii}^{00} = \boldsymbol{I}_{ii}^{01} = \boldsymbol{I}_{ii}^{10} = \boldsymbol{I}_{ii}^{11} = \boldsymbol{0}.$$

For neighboring panels, when $i = j + 1$ ($\boldsymbol{p}_2 = \boldsymbol{0}$, $\boldsymbol{s}_1 \neq \boldsymbol{0}$), coefficients α_3 and λ_3 vanish. For the other neighboring case, when $j = i + 1$ ($\boldsymbol{s}_1 = \boldsymbol{0}$, $\boldsymbol{p}_2 \neq \boldsymbol{0}$), coefficients α_1 and λ_1 should be equal to zero.

6. Conclusion

We derive exact analytical formulae for computing the integrals that arise in 2D vortex methods during simulating the flow around airfoils in hydrodynamic and coupled hydroelastic problems. These formulae are suitable for arbitrary airfoils when their surface lines are approximated by rectilinear panels. The distribution of known or unknown intensities of vortex or source sheets over the panels can be piecewise-constant or piecewise-linear, and either collocation-type or finite element-type methods can be used for solving boundary integral equations. Implementing a similar approach with higher-order basis functions (in particular, piecewise-quadratic) is unreasonable since it would not lead to achieving higher accuracy. Further improvement of the algorithm is possible only by taking into account the curvilinearity of the panels, for example, by using a least squares approach [17].

Usage of the derived formulae makes it possible to raise significantly the accuracy of computing the vortex sheet intensity and to improve the quality of velocity and vorticity field representation, especially, in proximity to the surface line of the airfoil.

Acknowledgement

This work is supported by the Russian Science Foundation (grant 17-79-20445).

References

[1] Lifanov I 1996 *Singular Integral Equations and Discrete Vortices* (Utrecht: VSP)
[2] Cottet G-H and Koumoutsakos P 2000 *Vortex Methods: Theory and Practice* (Cambridge: CUP)
[3] Lewis R 2005 *Vortex Element Methods for Fluid Dynamic Analysis of Engineering Systems* (Cambridge: CUP)
[4] Dynnikova G 2003 *Fluid Dynamics* **38** 670
[5] Dynnikova G 2004 *Doklady Physics* **49** 648
[6] Kuzmina K, Marchevsky I and Moreva V 2015 *Procedia Computer Science* **66** 73
[7] Chorin A 1973 *J. Fluid Mech.* **57** 785
[8] Degond P and Mas-Gallic S 1989 *Math. Comp.* **53** 485
[9] Ogami Y and Akamatsu T 1991 *Computers & Fluids* **19:3–4** 433
[10] Tokaty G 1994 *A History and Philosophy of Fluid Mechanics* (Dover: Courier Corporation)
[11] Lighthill M 1963 *Boundary Layer Theory* ed J Rosenhead (Oxford: OUP) Introduction pp 54–61
[12] Anronov P, Guvernuk S and Dynnikova G 2006 *Vortex Methods for Computation of Unsteady Hydrodynamic Loads* (Moscow: Moscow State University Press)
[13] Kuzmina K and Marchevsky 2015 *Proc. 4th Int. Conf. on Particle-Based Methods – Fundamentals and Applications, PARTICLES 2015 (Barcelona)* (Barcelona: Int. Center for Numerical Methods in Engineering (CIMNE)) p 680
[14] Saffman P 1992 *Vortex Dynamics* (Cambridge: CUP)
[15] Moreva V and Marchevsky I 2012 *ECCOMAS 2012 – European Congress on Computational Methods in Applied Sciences and Engineering, e-Book Full Papers (Vienna)* (Barcelona: Int. Center for Numerical Methods in Engineering (CIMNE)) p 5952
[16] Kuzmina K, Marchevskii I and Ryatina E 2017 *Russian Aeronautics* **60**
[17] Kuzmina K and Marchevsky I 2016 *Herald of the Bauman Moscow State Technical University, Series Natural Sciences* **69** 93